Increasing Exposure of the Petrous Internal Carotid Artery for Revascularization Using the Transzygomatic Extended Middle Fossa Approach: A Cadaveric Morphometric Study

James K. Liu, M.D.
Department of Neurosurgery,
University of Utah
School of Medicine,
Salt Lake City, Utah

Takanori Fukushima, M.D., D.M.Sc.
Carolina Neuroscience Institute,
Raleigh, North Carolina

Tetsuro Sameshima, M.D., Ph.D.
Carolina Neuroscience Institute,
Raleigh, North Carolina

Ossama Al-Mefty, M.D.
Department of Neurosurgery,
University of Arkansas,
Little Rock, Arkansas

William T. Couldwell, M.D., Ph.D.
Department of Neurosurgery,
University of Utah
School of Medicine,
Salt Lake City, Utah

Reprint requests:
William T. Couldwell, M.D., Ph.D.,
Department of Neurosurgery,
University of Utah,
30 North 1900 East, Suite 3B409,
Salt Lake City, UT 84132.
Email: william.couldwell@hsc.utah.edu

Received, January 19, 2006.
Accepted, May 31, 2006.

OBJECTIVE When internal carotid artery (ICA) sacrifice is planned in the management of difficult tumors or aneurysms at the cranial base, the petrous ICA may be a useful site for anastomosis for interpositional vascular bypass. However, exposure of the artery and performing an anastomosis in this region may be technically challenging because of the narrow working corridor. The authors describe a transzygomatic extended middle fossa approach that maximizes the exposure of the petrous ICA for performing the difficult anastomosis.

METHODS: Bilateral dissections were performed on eight silicone-injected cadaveric head specimens. Exposure of the entire petrous ICA (horizontal segment, genu, and vertical segment) using the transzygomatic extended middle fossa approach was performed by the following steps. A frontotemporal craniotomy was performed followed by a zygomatic osteotomy. The temporal lobe dura was elevated extradurally to expose the posterior cavernous sinus and floor of the middle fossa. The middle fossa rhomboid was identified, which is bordered by V3 anteriorly, the GSPN laterally, the arcuate eminence posteriorly, and the petrous edge medially. Bone drilling was performed in the middle fossa rhomboid and Glasscock's triangle with care not to violate the cochlea. The horizontal and vertical segments of the petrous ICA were skeletonized entirely and mobilized from carotid canal. The V3 segment of the trigeminal nerve was retracted anteriorly to obtain more distal exposure of the ICA. An osteoplastic bone flap of the middle fossa floor lateral to the ICA was removed to increase the working space. A morphometric analysis was performed, quantifying the petrous ICA exposure, the surgical working corridor, and the angles of exposure.

RESULTS: On average, the length of the horizontal petrous ICA exposed was 9.2 ± 1.0 mm (range, 8.0–11.0 mm). Anterior retraction of V3 provided an additional 4.3 ± 0.4 mm of carotid exposure (46.7% increase; $P < 0.05$). The length of the genu was on average 3.6 ± 0.4 mm (range, 3.0–4.0 mm), and the length of the vertical segment of the petrous ICA was 13.1 ± 2.0 mm (range, 10.0–15.0 mm). The average depth of the petrous ICA from the outer surface of the temporal bone was 30.6 ± 1.1 mm (range, 30.0–33.0 mm) at the V3–ICA junction and 27.2 ± 0.7 mm (range, 26.0–28.0 mm) at the ICA genu. The average diameter of the inner working corridor was 24.2 ± 3.0 mm (range, 21.5–30.0 mm). Removal of the zygoma increased the outer working corridor from an average distance of 24.4 ± 3.8 mm to 33.4 ± 3.4 mm (36.9% increase in exposure; $P < 0.05$). The average angle of exposure was 66.5% greater ($P < 0.05$) with zygomatic arch removal (39.3 ± 4.9 degrees) than without zygomatic arch removal (23.6 ± 2.7 degrees).

CONCLUSION: The transzygomatic extended middle fossa approach provides a wide surgical corridor for maximal exposure of the petrous ICA with minimized temporal lobe retraction. This large exposure facilitates vascular anastomoses at the petrous ICA and provides working room to maneuver instruments. The middle fossa rhomboid is a key landmark to identify the petrous ICA and to avoid neuro-otologic structures.

KEY WORDS: Cerebral revascularization, Cranial base tumors, Giant aneurysms, Interpositional vein bypass

Neurosurgery 59[ONS Suppl 4]:ONS-309–ONS-319, 2006 DOI: 10.1227/01.NEU.0000232638.96933.A0

Cerebral revascularization is an important strategy in the surgical management of complex cranial base tumors and aneurysms (4–6, 9, 10, 12). Patients who harbor complex aneurysms that cannot be clipped directly and who do not tolerate parent vessel occlusion may require a cerebrovascular bypass. In cases where cranial base tumors encase the carotid artery and an oncological resection is desired, a high-flow interpositional bypass may be necessary in planned carotid occlusion or sacrifice. Several high-flow bypass strategies using saphenous vein reconstruction have been described, including the cervical-to-petrous internal carotid artery (ICA), petrous-to-supraclinoid ICA, cervical-to-supraclinoid ICA, and cervical-to-M2 bypasses (3, 8, 11, 12, 14). These revascularization techniques are important tools in the surgical treatment of complex aneurysms and tumors of the cranial base and cavernous sinus.

The petrous-to-supraclinoid ICA bypass was first performed by Fukushima in 1986 to trap a giant cavernous aneurysm (unpublished; *Figs. 1* and 2). This technique later was elaborated on in the literature by Spetzler et al. (14) and Sekhar et al. (12). This bypass strategy provides a high-flow bypass that is entirely intracranial and avoids stress on the graft associated with head and neck movements. The length of the interpositional graft is also short, which minimizes the risk of delayed thrombosis. Nevertheless, the petrous-to-supraclinoid ICA bypass is one of the most technically challenging bypasses to perform because of the small working space and the deep and narrow subtemporal corridor. These make it difficult to maneuver the instruments for performing the proximal anastomosis at the petrous ICA. In the standard approach described in the original publication (14), a frontotemporal craniotomy is performed and approximately 10 to 12 mm of the horizontal segment of the petrous ICA is exposed by the removal of bone in Glasscock's triangle.

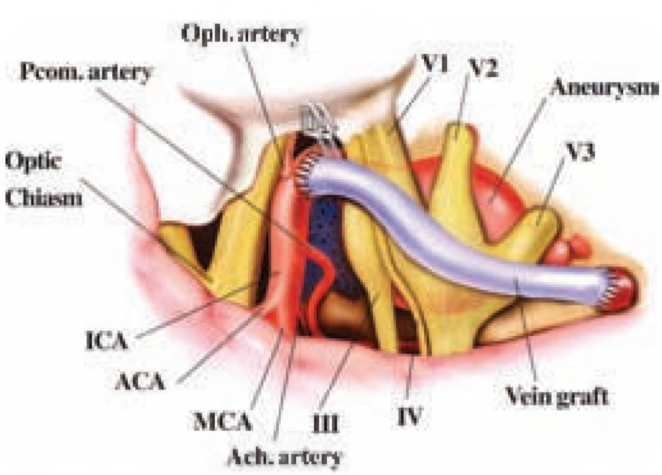

FIGURE 1. *Illustration demonstrating the petrous-to-supraclinoid internal carotid artery (ICA) bypass with an interpositional saphenous vein graft for a giant cavernous ICA aneurysm through a right-sided frontotemporal craniotomy exposure.* Oph. artery, *ophthalmic artery;* Pcom artery, *posterior communicating artery;* ACA, *anterior cerebral artery;* MCA, *middle cerebral artery;* Ach. artery, *anterior choroidal artery;* III, *oculomotor nerve;* IV, *trochlear nerve (with permission from, Fukushima T: Manual of skull base dissection. Raleigh, AF-Neurovideo, Inc., 2004, ed 2 [4]).*

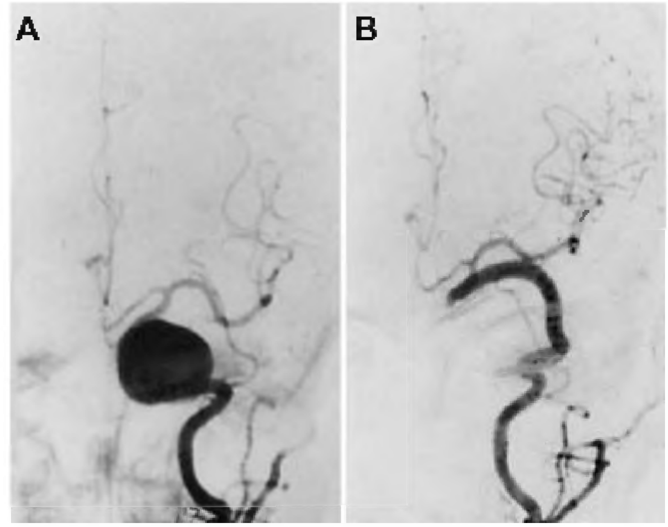

FIGURE 2. *Anteroposterior angiograms obtained before surgery (A) and after surgery (B) in a patient who underwent a petrous-to-supraclinoid internal carotid artery (ICA) bypass with an interpositional saphenous vein graft for a giant cavernous ICA aneurysm.*

We describe a transzygomatic extended middle fossa approach that increases the surgical corridor and maximizes exposure of the entire petrous ICA to facilitate the proximal anastomosis. This approach incorporates a zygomatic osteotomy, anterior mobilization of V3, and more extensive bone drilling of the middle fossa cranial base to provide total exposure of the horizontal and vertical segments of the petrous ICA. It also allows transposition of the petrous ICA from the carotid canal. A cadaveric morphometric analysis was performed to quantify the surgical exposure gained by performing the transzygomatic extended middle fossa approach versus the standard approach.

MATERIALS AND METHODS

Cadaver Preparation

Eight fresh cadaveric heads were prepared by soaking them in methanol for 24 hours and then in 10% formalin for another 24 hours. The carotid arteries and internal jugular veins were cannulated and injected with colored latex solution (Ward's Natural Science Est., Inc., Rochester, NY). The specimens then were placed in 10% formalin for another 24 hours. Bilateral dissections were performed on each cadaver head for a total of 16 sides. Anatomic dissections were performed at the University of Utah Skull Base Microsurgical Laboratory using a surgical microscope (Leica Microsystems Group, Wetzlar, Germany), standard microsurgical instruments, and a high-speed drill (Midas Rex, L.P., Fort Worth, TX).

Surgical Description

Exposure of the entire petrous ICA (horizontal segment, genu, and vertical segment) using the transzygomatic extended middle fossa approach can be simplified into the following six steps: 1) frontotemporal craniotomy, 2) zygomatic osteotomy, 3) extradural exposure of middle fossa and posterior cavernous sinus, 4) bone drilling of the middle fossa rhomboid, 5) bone drilling of Glasscock's triangle, 6) complete skeletonization and transposition of the entire petrous ICA. This final portion of the operation allows maximal exposure of the petrous ICA for the proximal anastomosis.

Exposure of the supraclinoid ICA remains unchanged from the standard approach. The sylvian fissure is opened widely. The anterior clinoid process is removed to expose the clinoidal segment of the ICA. The distal dural ring is opened to allow adequate exposure to place a clip on the ICA proximal to the ophthalmic artery. An interpositional vein graft is anastomosed to the petrous ICA proximally and to the supraclinoid ICA distally. A more detailed description of the bypass technique can be found in Spetzler et al. (13). The cadaveric dissections and morphometric analysis focus on the six steps mentioned above for maximizing exposure of the petrous ICA.

Dissection Technique

Step 1: Frontotemporal Craniotomy

The head is maintained in a three-pin head holder and is turned 45 degrees to the contralateral side. The malar eminence is positioned so that it is the highest point. A frontotemporal incision is made and a subfascial dissection of the temporalis muscle is performed to expose the orbit and zygoma while protecting the frontotemporal branch of the facial nerve (1, 15) (*Fig. 3*). A standard frontotemporal craniotomy is performed. The sphenoid wing is removed extradurally with rongeurs and a high-speed drill.

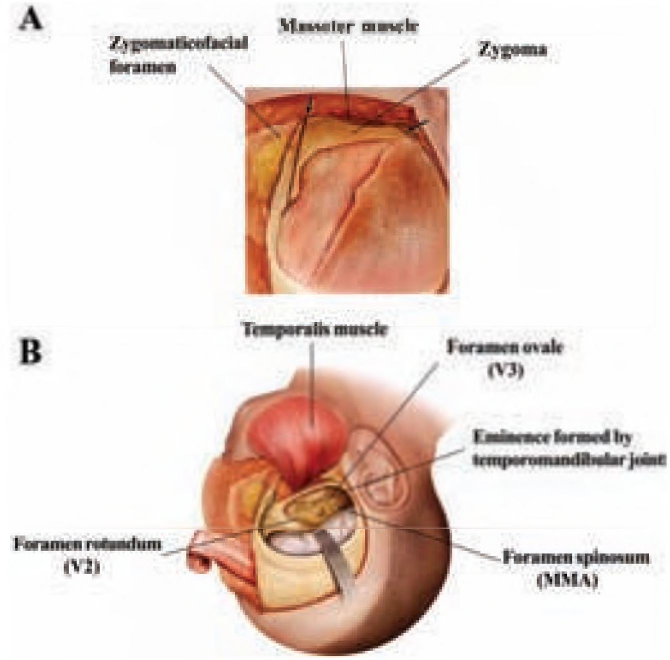

FIGURE 4. A, *illustration demonstrating where the bone cuts are made for the zygomatic osteotomy.* B, *illustration showing the exposure after performing the frontotemporal craniotomy and zygomatic osteotomy. The temporal lobe dura is elevated extradurally to expose the floor of the middle fossa.* MMA, *middle meningeal artery (with permission from, Fukushima T: Manual of skull base dissection. Raleigh, AF-Neurovideo, Inc., 2004, ed 2 [4]).*

Step 2: Zygomatic Osteotomy

Two cuts are made in the zygomatic arch. These cuts should be oblique to allow cosmetic reattachment. The first cut is made through the root of the zygoma just anterior to the temporomandibular joint and glenoid fossa. The second cut is made parallel to the lateral orbital rim, beginning at the frontozygomatic suture, leaving as little bone overhanging the frontozygomatic recess as possible. The arch can be displaced downward while preserving the attachments to the masseter muscle, or the arch can be freed from the masseter attachments (*Fig. 4*). Alternatively, a full orbitozygomatic osteotomy, as described by Zabramski et al. (15), can be performed if needed for the given pathological features. The temporalis muscle then is retracted inferiorly to expose the infratemporal fossa. The remainder of the squamous temporal bone is removed so that

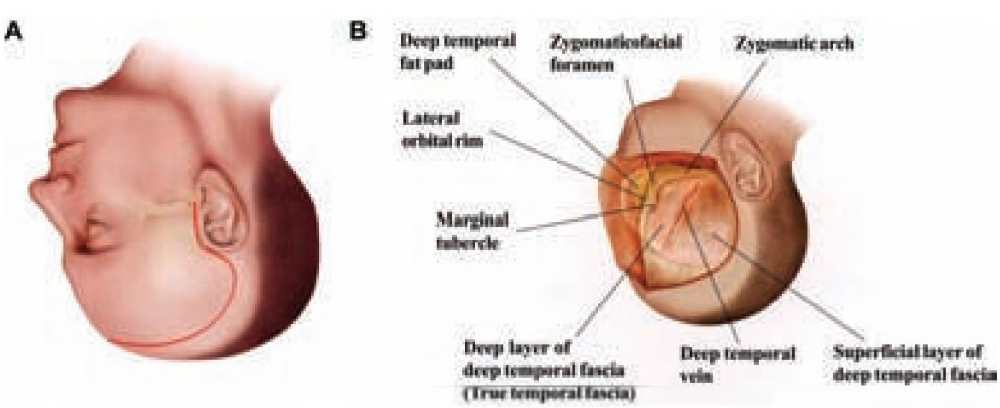

FIGURE 3. A, *illustration showing skin incision for the transzygomatic extended middle fossa approach.* B, *illustration showing subfascial dissection of the temporalis muscle to expose the zygoma while protecting the frontotemporal branch of the facial nerve (with permission from, Fukushima T: Manual of skull base dissection. Raleigh, AF-Neurovideo, Inc., 2004, ed 2 [4]).*

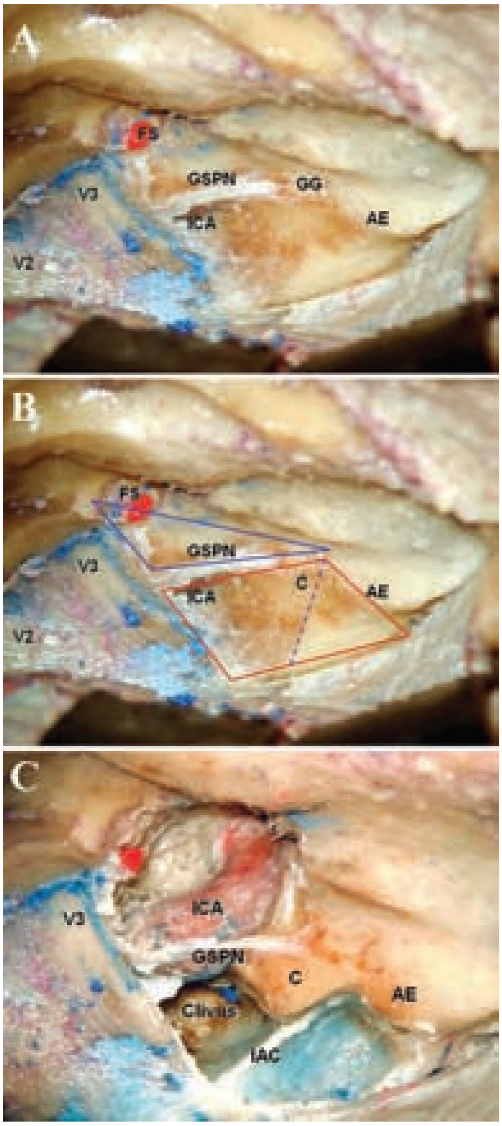

FIGURE 5. A, *cadaveric dissection (right-sided approach) photograph demonstrating the anatomy of the middle fossa. The temporal lobe is elevated extradurally to expose the floor of the middle fossa. This is performed in a posterior-to-anterior direction to avoid traction injury to the facial nerve by putting stretch on the greater superficial petrosal nerve (GSPN). The horizontal segment of the petrous internal carotid artery (ICA) is visible through a bony dehiscence. The arcuate eminence (AE) initially is identified along the petrous ridge. Extradural elevation then is continued anteromedially to expose the geniculate ganglion (GG) and the GSPN. The middle meningeal artery at the foramen spinosum (FS) is divided to allow further release of the temporal dura from the middle fossa cranial base to expose the posterior cavernous sinus and the V2 and V3 branches of the trigeminal nerve.* B, *cadaveric dissection photograph showing the middle fossa rhomboid* (red) *is bordered by V3 anteriorly, the GSPN laterally, the arcuate eminence posteriorly, and the petrous edge medially. The horizontal segment of the petrous ICA courses parallel to and beneath the GSPN. The internal auditory canal (IAC;* blue dotted line*) lies approximately in the plane that bisects the angle between the GSPN and AE. The cochlea* (C) *is situated anteromedial and inferior to the geniculate ganglion. Glasscock's triangle (*blue*) is bordered by the posterior rim of the foramen ovale, the foramen spinosum, the posterior border of V3, and the cochlear apex.* C, *cadaveric dissection photograph showing exposure of the petrous ICA after removal of bone in the middle fossa rhomboid and Glasscock's triangle.*

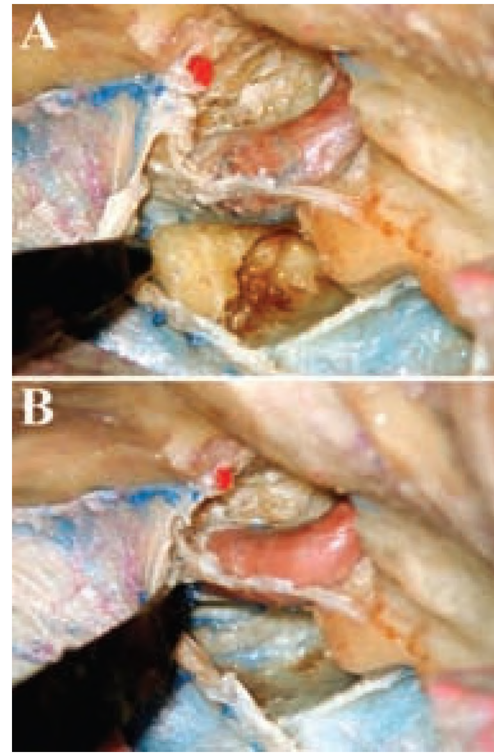

FIGURE 6. A, *cadaveric dissection photograph demonstrating anterior retraction of V3 to expose more bone at the petrous apex and more length of the horizontal petrous internal carotid artery (ICA).* B, *cadaveric dissection photograph showing that bone of petrous apex has been drilled away and additional exposure of the horizontal petrous ICA is achieved.*

the edge of the craniotomy is flush with the floor of the middle fossa to provide a flat trajectory across the floor.

Step 3: Extradural Exposure of the Middle Fossa and Posterior Cavernous Sinus

The temporal lobe is elevated extradurally to expose the floor of the middle fossa (*Fig. 5*). This is performed in a posterior-to-anterior direction while taking care to avoid traction injury to the facial nerve by putting stretch on the greater superficial petrosal nerve (GSPN) as it is separated from the dura. The arcuate eminence initially is identified along the petrous ridge. Extradural elevation then is continued anteromedially to expose the region of the geniculate ganglion and the GSPN, which lies in the major petrosal groove and is covered by a layer of connective tissue. The middle meningeal artery at the foramen spinosum is identified, coagulated, and divided to allow further release of the temporal dura from the middle fossa cranial base. The dura propria can now be elevated off the lateral wall of the cavernous sinus to expose the

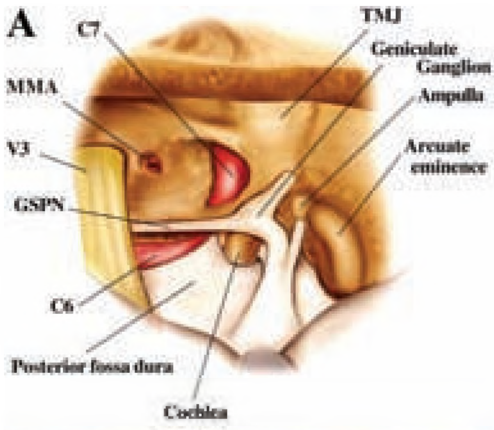

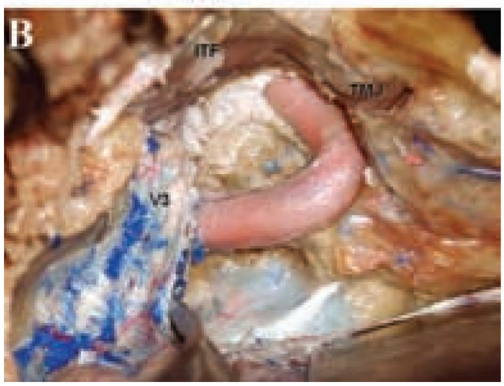

FIGURE 7. A, *illustration demonstrating exposure of the horizontal (C6) and vertical (C7) segments of the petrous internal carotid artery (ICA). Care is taken to avoid injury to the temporomandibular joint (TMJ).* GSPN, *greater superficial petrosal nerve;* MMA, *middle meningeal artery (with permission from, Fukushima T: Manual of skull base dissection. Raleigh, AF-Neurovideo, Inc., 2004, ed 2 [4]).* B, *cadaveric dissection photograph showing exposure of the entire petrous ICA from the horizontal segment to the genu and to the vertical segment. The horizontal segment of the ICA is exposed circumferentially in a 270-degree fashion. The anterior and lateral aspects of the vertical segment of the petrous ICA are unroofed completely down to the carotid canal entrance at the cranial base. The middle fossa cranial base lateral to the horizontal segment and anterior to the vertical segment has been removed to reveal the infratemporal fossa (ITF) contents. Care is taken not to injure the temporomandibular joint (TMJ) located posterior and lateral to the genu and vertical segment.*

mandibular division of the trigeminal nerve (V3) as it exits the foramen ovale. The medial extent of the dissection is the petrous ridge. The anatomic landmarks for the middle fossa rhomboid structure (2) can now be identified. The four points of the rhomboid are: 1) the intersection of the GSPN with the trigeminal nerve, 2) the porus trigeminus, 3) the intersection of the arcuate eminence and petrous ridge, and 4) the intersection of the lines projected along the axes of the GSPN and arcuate eminence. The horizontal segment of the petrous ICA may be visible through a bony dehiscence in the floor of the middle fossa in some cases. V3 is retracted anteriorly with a self-retaining retractor blade to provide more exposure of the middle fossa floor (*Fig. 6*).

Step 4: Bone Drilling of the Middle Fossa Rhomboid

The bone of the middle fossa rhomboid is removed in a stepwise fashion using a high-speed diamond burr and copious irrigation. Bone initially is removed by unroofing the medial two-thirds of the internal auditory canal (IAC), which lies in the bisection of the angle formed by the GSPN and the arcuate eminence. The dura overlying the IAC is identified and will flare at the porus acusticus. Bone anterior to the IAC then is removed toward V3 and the porous trigeminus. Anterior retraction of V3 facilitates total removal of the petrous apex and more exposure of the petrous ICA (*Fig. 6*). Bone is removed inferiorly and medially until the inferior petrosal sinus is exposed. It is important to avoid damage to the cochlea, which is located anteromedial and inferior to the geniculate ganglion. The bone between the IAC and the arcuate eminence then is removed.

The middle fossa rhomboid can be divided further into three triangles: Kawase's triangle, the premeatal triangle, and the postmeatal triangle (2). Kawase's triangle is defined laterally by the GPSN and medially by the petrous ridge. The base is formed by V3. The premeatal triangle is bounded by the medial lip of the internal acoustic meatus, the carotid genu, and the geniculate ganglion. This triangle identifies the precise location of the cochlea when drilling the petrous apex or exposing the intrapetrous carotid artery through the middle fossa. The cochlea is located in the lateral half of this triangle. The postmeatal triangle is bordered by the lateral lip of the internal acoustic meatus, the geniculate ganglion, and the intersection of the arcuate eminence with the petrous ridge. This is the region of bone that lies between the IAC and the superior semicircular canal.

Step 5: Bone Drilling of Glasscock's Triangle

Attention then is directed toward removal of bone overlying Glasscock's triangle, which is formed by the posterior rim of the foramen ovale, the foramen spinosum, the posterior border of V3, and the cochlear apex. The GSPN is transected here to prevent traction injury on the facial nerve. The horizontal segment of the petrous ICA is exposed. Anterior retraction of V3 allows additional distal exposure of the horizontal segment.

Step 6: Complete Skeletonization and Transposition of the Petrous ICA

The entire petrous ICA is skeletonized completely from the horizontal segment to the genu and to the vertical segment (*Fig. 7*). The middle fossa cranial base lateral to the horizontal segment and anterior to the vertical segment is flattened and thinned down with a high-speed drill. Alternatively, at this juncture, this region of the middle fossa can be removed via an osteoplastic bone flap (*Fig. 8*). Subperiosteal dissection is performed on the infratemporal surface of the middle fossa cranial base to separate the infratemporal fossa contents from the cranial base. A craniotome is used to create an osteoplastic bone flap that is located posterior to V3, lateral to the horizontal segment of the petrous ICA, and anterior to the vertical segment of the petrous

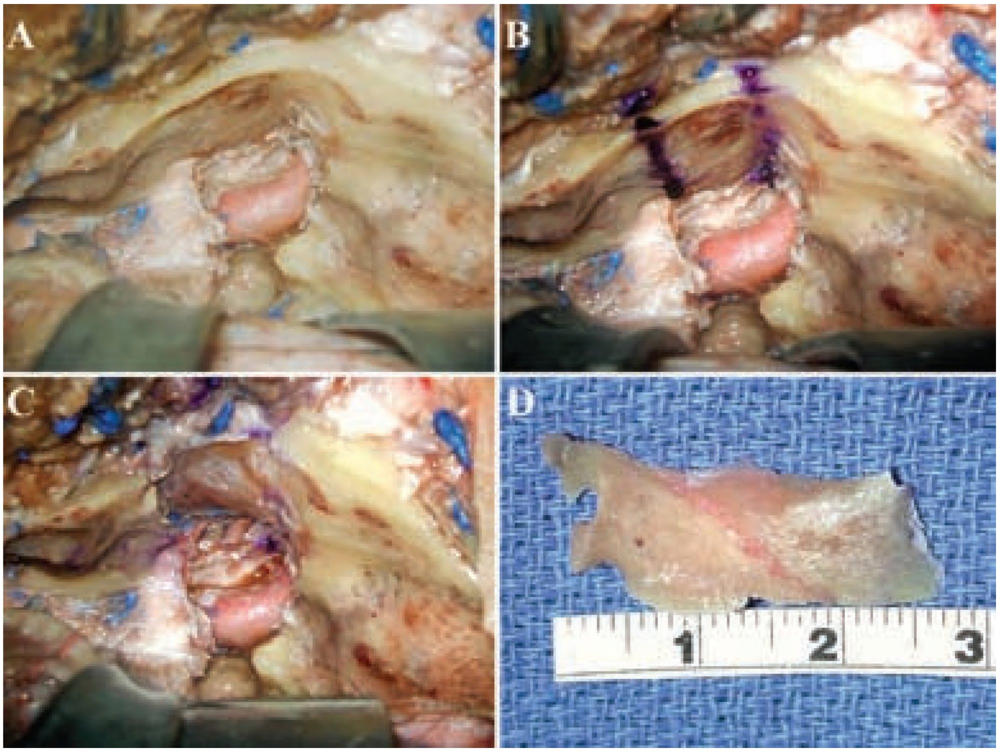

FIGURE 8. *Photographs demonstrating removal of middle fossa floor via an osteoplastic bone flap (right-sided approach). A, surgical view of the middle fossa using the transzygomatic extended middle fossa approach. The horizontal segment of the petrous internal carotid artery (ICA) has been exposed. The bony floor of the middle fossa lateral to the ICA has been flattened with a high-speed drill. B, same view demonstrating the region of bone (highlighted in* blue ink*) to be removed. C, same view demonstrating removal of the osteoplastic bone flap. A craniotome was used to create an osteoplastic bone flap that is located posterior to V3, lateral to the horizontal segment of the petrous ICA, and anterior to the vertical segment of the petrous ICA. It is important to stay anterior to the temporomandibular joint to avoid injury. The capsule of the infratemporal fossa contents is kept intact. D, photograph of the osteoplastic bone flap that was removed.*

ICA. It is important to stay anterior to the temporomandibular joint to avoid injury. The horizontal segment of the ICA is exposed circumferentially in a 270-degree fashion. The anterior and lateral aspects of the vertical segment of the petrous ICA are completely unroofed down to the carotid canal entrance at the cranial base. Drilling posterior to the genu and vertical segment can cause damage to the middle ear structures and the temporomandibular joint. As soon as the petrous ICA is decompressed from the bony carotid canal, it can be transposed and mobilized from the canal (*Fig. 9*). The Eustachian tube, which is located lateral to the horizontal segment of the petrous ICA, should be preserved if possible. If, however, it is entered, the Eustachian tube needs to be obliterated to prevent a cerebrospinal fluid leak. (The Eustachian tube has been removed in the photographs of the anatomic dissections for demonstration purposes.)

Morphometric Analysis

Quantification of Petrous ICA Exposure

The exposure of the petrous ICA was quantified to compare the standard approach versus the transzygomatic extended middle fossa approach. *Figure 10A* illustrates the anatomic references of the measurements. In the standard approach, only the horizontal segment of the petrous ICA is exposed (Measurement B) in Glasscock's triangle without anterior retraction of V3. In the transzygomatic extended middle fossa approach (anterior retraction of V3 and total petrous ICA exposure), the segments under V3 (Measurement A) and the genu (Measurement C) are exposed in addition to the horizontal segment. The entire vertical segment is exposed in the transzygomatic extended middle fossa approach, but not in the standard approach. The depth of the ICA from the outer surface of the temporal bone also was quantified.

Quantification of Surgical Working Corridors

The diameters of the inner and outer surgical working corridors were quantified to compare the standard approach versus the transzygomatic extended middle fossa approach. *Figure 10B* illustrates the anatomic references of the measurements. In the transzygomatic extended middle fossa approach, the inner working corridor was defined by the space lateral to the horizontal ICA (Measurement D), the width of the horizontal ICA (Measurement E), and the space medial to the ICA (Measurement F). In the standard approach, the inner surgical corridor was determined just by the width of the horizontal segment ICA (Measurement E). For both approaches, the outer surgical corridor was determined by the distance between the inferior edge of the temporal lobe and the superior edge of the inferiorly retracted temporalis muscle. In the extended approach, measurements were made with the zygoma removed, whereas in the standard approach, measurements were made with the zygoma replaced. Fixed temporal lobe retraction was maintained to allow consistency in measurements.

Quantification of Angles of Exposure

The angle of exposure was quantified using a goniometer. The midpoint of the horizontal segment of the petrous ICA served as apex of the angle (*Fig. 10C*). In the extended ap-

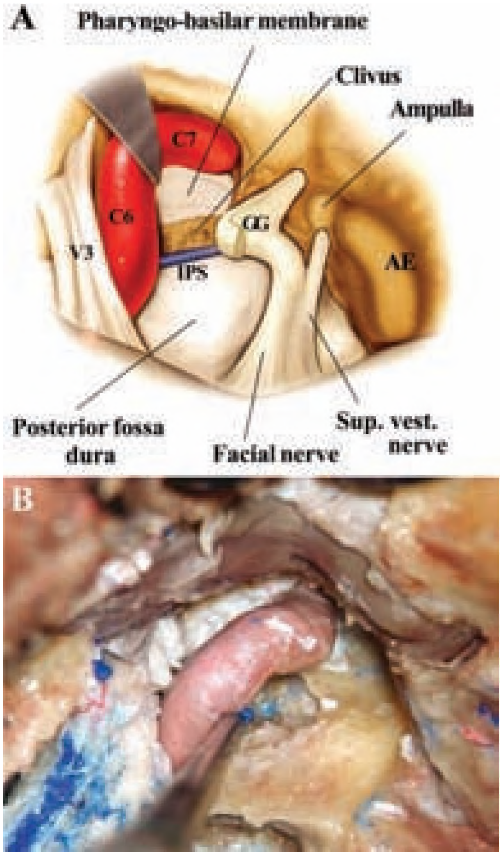

FIGURE 9. *Illustration* (A) *and cadaveric dissection photograph* (B) *showing transposition and mobilization of the petrous internal carotid artery (ICA) from its bony canal.* IPS, *inferior petrosal sinus;* GG, *geniculate ganglion;* AE, *arcuate eminence;* C6, *horizontal segment of ICA;* C7, *vertical segment of ICA;* Sup. vest. nerve, *superior vestibular nerve.* A, *(with permission from, Fukushima T: Manual of skull base dissection. Raleigh, AF-Neurovideo, Inc., 2004, ed 2 [4]).*

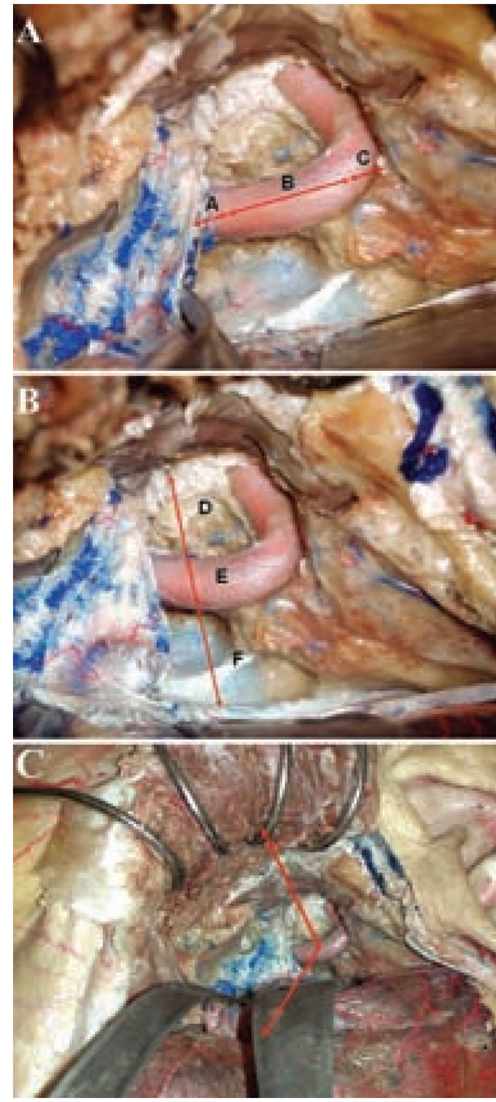

FIGURE 10. A, *measurements of the horizontal segment of the petrous internal carotid artery (ICA). Measurement A, segment of ICA under V3. Measurement B, horizontal segment of the petrous ICA that is exposed in Glasscock's triangle with the standard approach without anterior retraction of V3. Measurement C, genu.* B, *measurements of the inner surgical working corridor. In the transzygomatic extended middle fossa approach, the inner working corridor was defined by the space lateral to the horizontal ICA (Measurement D), the width of the horizontal ICA (Measurement E), and the space medial to the ICA (Measurement F). In the standard approach, the inner surgical corridor was determined just by the width of the horizontal segment ICA (Measurement E).* C, *quantification of angle of exposure. The midpoint of the horizontal segment of the petrous ICA served as the apex of the angle.*

proach, the angle was measured with the zygoma removed, whereas in the standard approach, the angle was measured with the zygoma replaced. Again, fixed temporal lobe retraction was maintained to allow consistency in measurements.

Statistical Analysis

The two-tailed, unpaired, Student's t test was used to compare the measurements and angles of exposure between the standard approach and the transzygomatic extended middle fossa approach. A P value of < 0.05 was considered statistically significant.

RESULTS

The morphometric analysis is summarized in *Tables 1* through *4* (*Fig. 10*). On average, the length of the horizontal petrous ICA exposed using the standard approach (Measurement B) was 9.2 ± 1.0 mm (range, 8.0–11.0 mm). When the transzygomatic extended middle fossa approach was used, the length of the horizontal petrous ICA exposed (Measurement A + B + C) was 17.1 ± 1.4 mm, which was a 85.9% increase in exposure ($P < 0.05$). Anterior retraction of V3 provided an additional 4.3 ± 0.4 mm of carotid exposure

(46.7% increase; $P < 0.05$). The length of the genu (Measurement C) was on average 3.6 ± 0.4 mm (range, 3.0–4.0 mm) and the vertical segment of the petrous ICA was 13.1 ± 2.0 mm (range, 10.0–15.0 mm). The average depth of the petrous ICA from the outer surface of the temporal bone was 30.6 ± 1.1 mm (range, 30.0–33.0 mm) at the V3–ICA junction and 27.2 ± 0.7 mm (range, 26.0–28.0 mm) at the ICA genu.

The average diameter of the inner working corridor for the standard approach (Measurement E) was 5.2 ± 0.4 mm (range, 5.0–6.0 mm). For the extended approach, the average diameter of the inner working corridor (Measurements D + E + F) was 24.2 ± 3.0 mm (range, 21.5–30.0 mm), which was a 365.4% increase in exposure ($P < 0.05$). Removal of the zygoma increased the outer working corridor from an average distance of 24.4 ± 3.8 mm (standard approach) to 33.4 ± 3.4 mm (extended approach), which was an overall 36.9% increase in exposure ($P < 0.05$).

The average angle of exposure was significantly greater with zygomatic arch removal in the extended approach (39.3 ± 4.9 degrees) when compared with the standard approach without zygomatic arch removal (23.6 ± 2.7 degrees). The overall increase in the angle of exposure achieved by the transzygomatic extended middle fossa approach was 66.5% ($P < 0.05$).

TABLE 1. Quantification of the horizontal segment of the petrous internal carotid artery

Measurement label[a]	Corresponding anatomical references	Length (mm; range)
A	V3	4.3 ± 0.4 (4.0–5.0)
B	Internal carotid artery (standard approach)	9.2 ± 1.0 (8.0–11.0)
C	Genu	3.6 ± 0.4 (3.0–4.0)
A + B + C	Total length	17.1 ± 1.4 (15.5–19.5)

[a] See *Figure 10A* for illustration.

TABLE 2. Increased exposure of the horizontal segment of the petrous internal carotid artery[a]

Measurement label[b]	Corresponding anatomical references	Percent increase in ICA exposure
A + B	V3 + ICA	46.7% ($P < 0.05$)
B + C	ICA + genu	39.1% ($P < 0.05$)
A + B + C	V3 + ICA + genu	85.9% ($P < 0.05$)

[a] ICA, internal carotid artery.
[b] See *Figure 10A* for illustration.

TABLE 3. Quantification of the inner working corridor[a]

Measurement label[b]	Corresponding anatomical references	Length (mm; range)
D	Space lateral to ICA	9.3 ± 2.1 (7.0–13.0)
E	ICA width	5.2 ± 0.4 (5.0–6.0)
F	Space medial to ICA	9.9 ± 1.4 (8.0–12.0)
D + E + F	Total length	24.2 ± 3.0 (21.5–30.0)

[a] ICA, internal carotid artery.
[b] See *Figure 10B* for illustration.

DISCUSSION

Clinical Experience with the Petrous-to-supraclinoid ICA Bypass

Since the development of the petrous-to-supraclinoid ICA bypass by Fukushima in the mid-1980s, two of the senior authors (TF, WTC) have had considerable experience with the bypass. The advantages of the bypass are that it limits the length of the bypass to the shortest possible for bypassing lesions of the cavernous sinus, it provides immediate high flow with a large-caliber conduit, and it is entirely within the head. This revascularization strategy has the advantages of minimal kinking of the graft from head and neck torsion and an overall shortened graft length, factors that help promote graft patency (10, 11). However, in the authors' opinion, the bypass is one of the most challenging in vascular neurosurgery, given the location of the proximal and distal anastomosis. Performing an anastomosis at

TABLE 4. Comparison of exposure between standard and extended approaches

Measurement	Standard approach	Extended approach	Percent increase in exposure
Inner working corridor	5.2 ± 0.4 mm	24.2 ± 3.0 mm	365.4% ($P < 0.05$)
Outer working corridor	24.4 ± 3.8 mm	33.4 ± 3.4 mm	36.9% ($P < 0.05$)
Angle of exposure	23.6 ± 2.7 degrees	39.3 ± 4.9 degrees	66.5% ($P < 0.05$)

the petrous ICA using the standard approach without zygoma removal and extended middle fossa drilling can be difficult because of the small working space and the deep and narrow subtemporal corridor, making it difficult to maneuver the instruments for performing microanastomosis.

The petrous-to-supraclinoid ICA bypass has been performed a total of 59 times by the two authors for cases of giant cavernous aneurysm (45 patients), meningioma involving the cavernous carotid (10 patients), and other tumor pathological features (4 patients). The bypasses have remained patent in 48 out of 49 cases at last follow-up (range, 1–20 yr) and have been complicated by transient postoperative ischemic deficit in two cases and variable amounts of visual loss in the ipsilateral eye in four cases (6.7%). This latter problem is the major risk of the bypass and likely results from temporary occlusion of the ophthalmic artery while performing the bypass. Thus, the present anatomic study was undertaken in an effort to facilitate exposure of the carotid to perform the bypass with the shortest possible occlusion time (without extended middle fossa exposure, the anastomosis optimally takes 30–40 min).

Advantages of Increased Exposure for Revascularization

The transzygomatic extended middle fossa approach described here provides maximal exposure of the entire petrous ICA, from the carotid canal at the cranial base to the cavernous sinus segment. This exposure is useful when considering a high-flow bypass with the petrous ICA as a site for anastomosis, as in the case of the petrous-to-supraclinoid ICA bypass.

Our extended approach maximizes the working corridors and angles of exposure for accessing the petrous ICA. Performing the zygomatic osteotomy increased the outer working corridor from 24.4 mm to 33.4 mm (36.9% increase; $P < 0.05$), whereas the extended middle fossa bone drilling increased the inner working corridor from 5.2 mm to 24.2 mm (365.4% increase; $P < 0.05$). These extensions maximize the overall working space to facilitate easier maneuverability of the tying instruments for performing microanastomosis in a deep hole. The geometrical working space expands from a narrow conical space to a wider cylindrical space (*Fig. 11*). Removal of the zygoma also facilitates maximal inferior mobilization of the temporalis muscle to provide a more basal trajectory to the petrous ICA and cranial base (*Fig. 12*). The angle of exposure also increased from 23.6 to 39.3 degrees (66.5% increase; $P < 0.05$) with this maneuver.

Another advantage of the transzygomatic extended middle fossa approach is that the entire length of the petrous ICA is exposed and can be transposed from the carotid canal. This provides maximal length of the petrous ICA and allows for multiple options for sites of anastomosis along the course of the entire petrous ICA. It also creates more space to place temporary clips on the artery. Mobilization and transposition of the petrous ICA from the bony carotid canal allows the surgeon to bring the artery up into a more optimal position for grafting. Freedom from the bony canal also facilitates the placement of sutures on the back side of the graft.

Standard Approach	Extended Approach
Inner cone: 5.2 mm Outer cone: 24.4 mm	Inner cone: 24.2 mm Outer cone: 33.4 mm

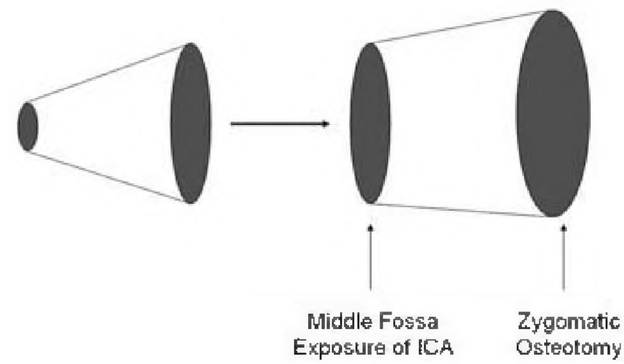

FIGURE 11. *Schematic diagram demonstrating the gain in exposure with the transzygomatic extended middle fossa approach. By removing the zygoma and performing extended middle fossa drilling, the geometrical working space expands from a narrow conical space to a wider cylindrical space.* ICA, *internal carotid artery.*

Microsurgical Anatomy of the Petrous ICA and Middle Fossa

The middle fossa cranial base contains several important neurovascular structures, including the petrous ICA, trigeminal nerve, GSPN, geniculate ganglion, facial nerve, cochlea, and superior semicircular canal. The middle fossa rhomboid, previously reported by Day et al. (2), is a useful landmark to identify the petrous ICA and for avoiding important neuro-otologic structures during bone drilling. This rhomboid structure is bordered by V3 anteriorly, the GSPN laterally, the arcuate eminence posteriorly, and the petrous edge medially. The horizontal segment of the petrous ICA courses parallel to and beneath the GSPN. The IAC lies approximately in the plane that bisects the angle between the GSPN and arcuate eminence. The cochlea is situated anteromedial and inferior to the geniculate ganglion. It is bordered by the genu of the petrous ICA anteriorly, the geniculate ganglion laterally, and the medial lip of the IAC posteriorly. Knowledge of the middle fossa rhomboid anatomy is important for avoiding injury to neighboring neurovascular structures during petrous bone drilling.

The petrous ICA enters the cranial base as the vertical segment at the carotid canal in the petrous portion of the temporal bone. The canal is lined by periosteum and is situated anterior to the jugular foramen. The vertical segment of the petrous ICA ascends directly upward after entering the petrous bone and turns anteromedially at the genu to form the horizontal segment. Our measurements of the petrous ICA were consistent with those reported by Paullus et al. (8). In our study, the average length of the vertical segment was 13.1 mm (range, 10–15 mm). The average diameter of the petrous ICA was 5.2 mm and there was no significant difference in the

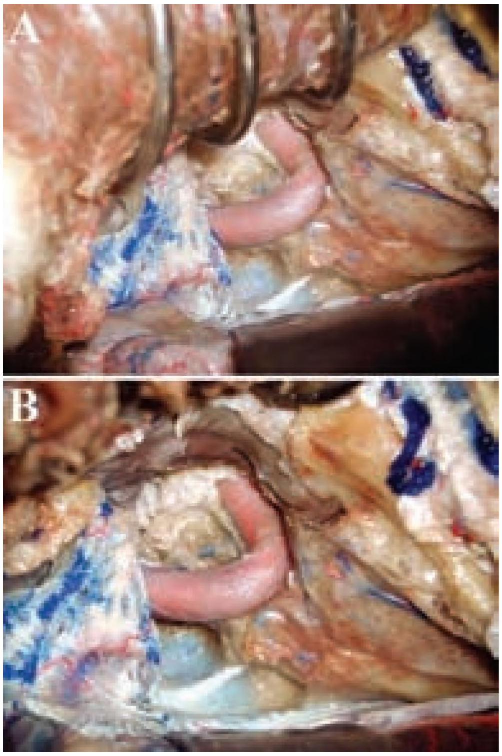

FIGURE 12. *Cadaveric dissection photographs demonstrating the exposure gained from removing the zygoma. A, exposure without removal of zygoma. B, exposure with removal of zygoma. Removal of the zygoma facilitates maximal inferior mobilization of the temporalis muscle to provide a more basal trajectory to the petrous internal carotid artery (ICA) and cranial base. This maneuver also increases the outer working corridor and the angle of exposure.*

diameter between the vertical and horizontal segments. The horizontal segment of the petrous ICA courses anteromedially towards V3. The cochlea lies posterior to the genu and is separated by a thin rim of bone. In approximately half of our specimens, a bony dehiscence protruded over the horizontal segment. The average length of the horizontal segment was 17.1 mm (range, 15–20 mm).

CONCLUSION

The transzygomatic extended middle fossa approach provides complete exposure of the petrous ICA from the cavernous sinus to the carotid canal at the cranial base. The surgical corridor is maximized to allow instrument maneuverability to facilitate proximal anastomosis at the petrous ICA. Knowledge of the middle fossa rhomboid construct is useful for safely locating the petrous ICA while avoiding injury to critical neuro-otological structures during bone drilling. Practice in the cadaver laboratory is necessary to familiarize the surgeon with the microsurgical anatomy.

REFERENCES

1. Coscarella E, Vishteh AG, Spetzler RF, Seoane E, Zabramski JM: Subfascial and submuscular methods of temporal muscle dissection and their relationship to the frontal branch of the facial nerve. Technical note. **J Neurosurg** 92:877–880, 2000.
2. Day JD, Fukushima T, Giannotta SL: Microanatomical study of the extradural middle fossa approach to the petroclival and posterior cavernous sinus region: Description of the rhomboid construct. **Neurosurgery** 34:1009–1016, 1994.
3. Fitzpatrick BC, Spetzler RF, Ballard JL, Zimmerman RS: Cervical-to-petrous internal carotid artery bypass procedure. Technical note. **J Neurosurg** 79: 138–141, 1993.
4. Fukushima T: *Manual of Skull Base Dissection.* Raleigh, AF-Neurovideo, Inc. 2004, ed 2.
5. Javedan SP, Deshmukh VR, Spetzler RF, Zabramski JM: The role of cerebral revascularization in patients with intracranial aneurysms. **Neurosurg Clin N Am** 12:541–555, viii, 2001.
6. Lawton MT, Hamilton MG, Morcos JJ, Spetzler RF: Revascularization and aneurysm surgery: Current techniques, indications, and outcome. **Neurosurgery** 38:83–94, 1996.
7. Lawton MT, Spetzler RF: Surgical strategies for giant intracranial aneurysms. **Acta Neurochir Suppl** 72:141–156, 1999.
8. Miyazaki S, Fukushima T, Fujimaki T: Resection of high-cervical paraganglioma with cervical-to-petrous internal carotid artery saphenous vein bypass. Report of two cases. **J Neurosurg** 73:141–146, 1990.
9. Paullus WS, Pait TG, Rhoton AL Jr: Microsurgical exposure of the petrous portion of the carotid artery. **J Neurosurg** 47:713–726, 1977.
10. Sekhar LN, Bucur SD, Bank WO, Wright DC: Venous and arterial bypass grafts for difficult tumors, aneurysms, and occlusive vascular lesions: Evolution of surgical treatment and improved graft results. **Neurosurgery** 44: 1207–1224, 1999.
11. Sekhar LN, Kalavakonda C: Cerebral revascularization for aneurysms and tumors. **Neurosurgery** 50:321–331, 2002.
12. Sekhar LN, Sen CN, Jho HD: Saphenous vein graft bypass of the cavernous internal carotid artery. **J Neurosurg** 72:35–41, 1990.
13. Sekhar LN, Stimac D, Bakir A, Rak R: Reconstruction options for complex middle cerebral artery aneurysms. **Neurosurgery** 56 [Suppl 1]:66–74, 2005.
14. Spetzler RF, Fukushima T, Martin N, Zabramski JM: Petrous carotid-to-intradural carotid saphenous vein graft for intracavernous giant aneurysm, tumor, and occlusive cerebrovascular disease. **J Neurosurg** 73:496–501, 1990.
15. Zabramski JM, Kiris T, Sankhla SK, Cabiol J, Spetzler RF: Orbitozygomatic craniotomy. Technical note. **J Neurosurg** 89:336–341, 1998.

Acknowledgments

We thank Kristin Kraus for her editorial assistance in preparing this manuscript and Stanley M. Coffman for the color illustrations.

COMMENTS

The authors describe the transzygomatic extended middle fossa approach for increasing the exposure of the petrous internal carotid artery (ICA) for bypass procedures. The technique requires a zygomatic osteotomy, anterior mobilization of the mandibular branch of the trigeminal nerve, extensive drilling of the middle fossa cranial base, and transposition of the petrous ICA from its bony canal. This extensive dissection maximizes the exposure of the petrous ICA, mobilizing the petrous segment from its entrance into the carotid canal to the cavernous segment. This additional exposure was quantified in cadaveric specimens, and the middle fossa drilling significantly increased the deep portion of the surgical corridor, widening it from a cone to a cylinder. This dissection is intended to facilitate the petrous ICA anastomosis in what is perhaps the most technically difficult intracranial bypass and, on the basis of the data and the beautiful illustrations presented, this approach succeeds. In addition to creating more room to maneuver instruments, the approach also creates more room for proximal and distal clips on the ICA, which can crowd the field. The authors have a combined experience with petrous bypasses in 59 patients, which is both remarkable and impressive.

My own experience with this bypass is more limited. I enjoy the technical challenge of the petrous-to-supraclinoid ICA bypass, but find that it is a bypass with few indications. I have used it exclusively in young patients in whom the advantages of its short length, increased long-term patency, and protected intracranial location justify the more extensive dissection and increased risks (1). These surgical risks are not trivial. The surgical field is densely packed with critical structures, and slight breaches in technique can produce deafness (penetration of the cochlea), blindness (optic nerve manipulation or ophthalmic artery occlusion), facial weakness (traction on the greater superficial petrosal nerve), facial numbness (retraction of the trigeminal nerve), or stroke (graft occlusion or embolization). Therefore, the technical difficulty and high risk of this bypass make simpler bypasses with lower risks more appealing, including the cervical carotid artery to middle cerebral artery bypass. I applaud the authors for giving us a new technique that makes the petrous-to-supraclinoid ICA bypass easier to perform. I add a note of caution to those considering using it: this technique demands appropriate clinical indications, practice on cadavers in the cranial base laboratory, and a high level of technical expertise.

Michael T. Lawton
San Francisco, California

1. Sanai N, Quinones-Hinojosa A, Gupta NM, Perry V, Sun PP, Wilson CB, Lawton MT: Pediatric intracranial aneurysms: Durability of treatment following microsurgical and endovascular management. **J Neurosurg** 104: 82–89, 2006.

Anastomoses involving the petrous ICA can be challenging because of the narrow surgical corridor. In this cadaveric study, Liu et al. undertook a morphometric analysis of the additional exposure of the petrous ICA gained with a maximal transzygomatic extended middle fossa approach as compared with a standard frontotemporal craniotomy and exposure of the petrous ICA solely within Glasscock's triangle. The authors concisely deconstruct the transzygomatic extended middle fossa approach into six steps: 1) frontotemporal craniotomy, 2) zygomatic osteotomy, 3) extradural middle fossa exposure, 4) drilling of the middle fossa rhomboid, 5) drilling of Glasscock's triangle, and 6) skeletonization and potential transposition of the entire petrous ICA segment. The authors demonstrate that the additional bone work significantly increases the anatomic working space directly encompassing the petrous ICA as well as the surgical corridor between the extradural temporal lobe and the inferiorly displaced temporalis muscle.

We routinely use the orbitozygomatic osteotomy when performing petrous ICA bypasses. The additional exposure of the petrous ICA gained with the extended transzygomatic middle fossa approach must be balanced with the increased intraoperative time and potential risk to the cochlea and eustachian tube. The quantitative data reported by the authors will prove useful in such surgical decision-making.

Robert F. Spetzler
Pankaj Gore
Phoenix, Arizona

The authors described the so-called transzygomatic middle fossa approach, which increases the working space for anastomoses to be realized on the intrapetrous carotid artery. They performed bilateral dissections on eight silicone-injected cadaveric head specimens and realized a morphometric analysis to quantify a petrous ICA could be increased from 9.2 to 17.1 mm (a difference of 86%) and even an additional 4.3 mm (a difference of 47%) by retracting the V3 root anteriorly. The angle of exposure gained through zygomatic arch removal increased from 23 to 39 degrees (67%). The authors concluded that zygomatic arch removal, extended middle fossa drilling, and anterior retraction of the V3 root significantly increased the working space around the intrapetrous carotid artery. This approach minimized temporal lobe retraction and will facilitate anastomoses in this technically highly difficult location.

This is a detailed presentation of a tricky exposure, which may be useful for everyone going to the cavernous sinus and to the petrous apex. In my experience, overall indications for extracranial-intracranial bypass are very rare, and I prefer to use the external to ICA or middle cerebral artery because it reduces the duration of ICA occlusion.

Bernard George
Paris, France

Liu et al. describe a transzygomatic extended middle fossa approach that maximizes the exposure of the petrous ICA. We think that a shorter graft has the advantage in its patency in general. However, exposure of the petrous ICA and performing an anastomosis in this region may be technically challenging because of the narrow working corridor. This approach provides maximal exposure of the entire petrous ICA (from the carotid canal at the cranial base to the cavernous sinus segment). We think that the method described in this article can improve the technical aspect of the petrous-to-supraclinoidal ICA bypass.

Yasushi Takagi
Nobuo Hashimoto
Kyoto, Japan